

Article

Development of an Acid-Labile Ketal Linked Amphiphilic Block Copolymer Nanoparticles for pH-Triggered Release of Paclitaxel

Svetlana Lukáš Petrova *, Eliézer Jäger, Alessandro Jäger *, Anita Höcherl, Rafał Konefał, Alexander Zhigunov, Ewa Pavlova, Olga Janoušková  and Martin Hrubý

Institute of Macromolecular Chemistry v.v.i., Academy of Sciences of the Czech Republic, Heyrovsky Sq. 2, 162 06 Prague, Czech Republic; jager@imc.cas.cz (E.J.); hocherl@imc.cas.cz (A.H.); konefal@imc.cas.cz (R.K.); zhigunov@imc.cas.cz (A.Z.); pavlova@imc.cas.cz (E.P.); janouskova324@gmail.com (O.J.); hruby@imc.cas.cz (M.H.)

* Correspondence: petrova@imc.cas.cz (S.L.P.); ajager@imc.cas.cz (A.J.);
Tel.: +420-296-809-296 (S.L.P.); +420-296-809-274 (A.J.)

Abstract: Here, we report on the construction of biodegradable poly(ethylene oxide monomethyl ether) (MPEO)-*b*-poly(ϵ -caprolactone) (PCL) nanoparticles (NPs) having acid-labile (acyclic ketal group) linkage at the block junction. In the presence of acidic pH, the nanoassemblies were destabilized as a consequence of cleaving this linkage. The amphiphilic MPEO-*b*-PCL diblock copolymer self-assembled in PBS solution into regular spherical NPs. The structure of self-assemble and disassemble NPs were characterized in detail by dynamic (DLS), static (SLS) light scattering, small-angle X-ray scattering (SAXS), and transmission electron microscopy (TEM). The key of the obtained NPs is using them in a paclitaxel (PTX) delivery system and study their in vitro cytostatic activity in a cancer cell model. The acid-labile ketal linker enabled the disassembly of the NPs in a buffer simulating an acidic environment in endosomal (pH ~5.0 to ~6.0) and lysosomal (pH ~4.0 to ~5.0) cell compartments resulting in the release of paclitaxel (PTX) and formation of neutral degradation products. The in vitro cytotoxicity studies showed that the activity of the drug-loaded NPs was increased compared to the free PTX. The ability of the NPs to release the drug at the endosomal pH with concomitant high cytotoxicity makes them suitable candidates as a drug delivery system for cancer therapy.

Keywords: MPEO-*b*-PCL nanoparticles; acyclic ketal group; paclitaxel; human HeLa carcinoma cells



Citation: Petrova, S.L.; Jäger, E.; Jäger, A.; Höcherl, A.; Konefał, R.; Zhigunov, A.; Pavlova, E.; Janoušková, O.; Hrubý, M. Development of an Acid-Labile Ketal Linked Amphiphilic Block Copolymer Nanoparticles for pH-Triggered Release of Paclitaxel. *Polymers* **2021**, *13*, 1465. <https://doi.org/10.3390/polym13091465>

Academic Editors: Hermis Iatrou and Juhyun Park

Received: 8 April 2021

Accepted: 28 April 2021

Published: 1 May 2021

Publisher's Note: MDPI stays neutral with regard to jurisdictional claims in published maps and institutional affiliations.



Copyright: © 2021 by the authors. Licensee MDPI, Basel, Switzerland. This article is an open access article distributed under the terms and conditions of the Creative Commons Attribution (CC BY) license (<https://creativecommons.org/licenses/by/4.0/>).

1. Introduction

Over the past two decades, amphiphilic block copolymers (composed of hydrophilic and hydrophobic blocks) have been extensively studied [1–5]. Because of their unique capability to self-assemble in aqueous media, they attract considerable interest as potential biomedical applications in drug delivery and in the gene transfection field [6–8]. One key feature of these materials is associated with their capability to bear the lipophilic agent (drug) and release it in a controlled manner [7,9]. However, these nanoassemblies consist of a compact core of the insoluble block, which works as a reservoir for drugs surrounded by a flexible corona of the soluble block and often shown the slow release profile of encapsulated molecules [10–13]. It is of particular importance that hydrophilic corona provides a highly water-bound barrier to ensure colloidal stability, reduction in the rate of opsonin adhesion, and uptake by cells of the reticuloendothelial system (RES), which prolongs blood circulation lifetime [10,14–16].

In addition, self-assembled NPs gain much more relevance in biomedical applications, especially if they are tailored to be degradable as a response to external stimuli. Such stimulus may be the enzymatic removal of protecting groups [16], light [17], temperature [18], redox gradient [19], or change of pH [20]. The degradation through stimuli-

responsive involving the cleavage of labile linkages in response to external stimuli has been widely studied as a promising platform for the enhanced/controlled release of encapsulated molecules [21,22]. To address this issue, the ability of such a system to generate a nanoparticle release of cargo at selective pH in response to the acidic tumor environment intracellularly triggered by endo/lysosomes has been extensively studied. Besides, the targeted delivery to tumors can be achieved through cleavage of these linkages at acidic tumor conditions (cancer cells and tumor tissues ranging from pH 5.7 to 7.2); the drug can be rapidly released accompanied by dissolution of nanocarriers [23,24].

Considering the high acidity in tumor tissues and intracellular compartments, several polymers responsive to pH-sensitive hydrolysis, enzymatic degradation, and/or redox reactions could be suitable for triggering drug release undergoing degradation to various extents in vitro and/or in vivo, acid-labile groups. Such acid-labile linkers, can be hydrazone [25], orthoester [26,27], imine [28], ketal, or acetal [29,30], which have often been used as a responsive group to construct pH-responsive (co)polymers [31,32]. Among all these mentioned above, acid-degradable (co)polymers that contain ketal/acetal labile linkers on the polymer backbone or as pendant groups enabling drug attachment and these NPs have received great interest due to their special features [33,34].

Among the various approaches reported to date, previously we have studied the introduction of acid-cleavable ketal linkage at the junction of poly(ϵ -caprolactone) (PCL) hydrophobic and poly(ethylene oxide) (PEO) hydrophilic blocks driven by the fact that could have great potential as a drug delivery system [29]. The choice of PCL and PEO as building blocks is due to their excellent biodegradability and biocompatibility. Indeed, PCL is aliphatic hydrophobic polyester; it has been approved by the food and drug administration (FDA) and widely used for biomedical applications [35,36]. Furthermore, PEO is a hydrophilic, water-soluble, and very flexible biocompatible polymer that is non-toxic and easily eliminated from the body [37].

The present study was undertaken to investigate the potential of MPEO-*b*-PCL block copolymer NPs as a tumor-specific drug delivery carrier (Figure 1). The cytotoxic drug paclitaxel (PTX) was chosen as a model hydrophobic drug to evaluate the loading and triggered release profiles of the NPs. PTX was encapsulated in the hydrophobic core by hydrophobic interactions. The drug release and cytotoxic activity of the novel NPs prepared from the MPEO₄₄-*b*-PCL₁₇ block copolymer were evaluated on human HeLa carcinoma cells in vitro. Due to the specific chemical structure of the block copolymer, NPs disassemble and release the drug cargo under mildly acidic conditions (which simulate the acidic environment in endosomal and lysosomal compartments), exerting in vitro cytostatic efficacy on HeLa human cervical carcinoma cell line. The hydrolysis of the ketal linkage results in neutral degradation products, which can be easily excreted, avoiding accumulation and likely inflammatory responses.

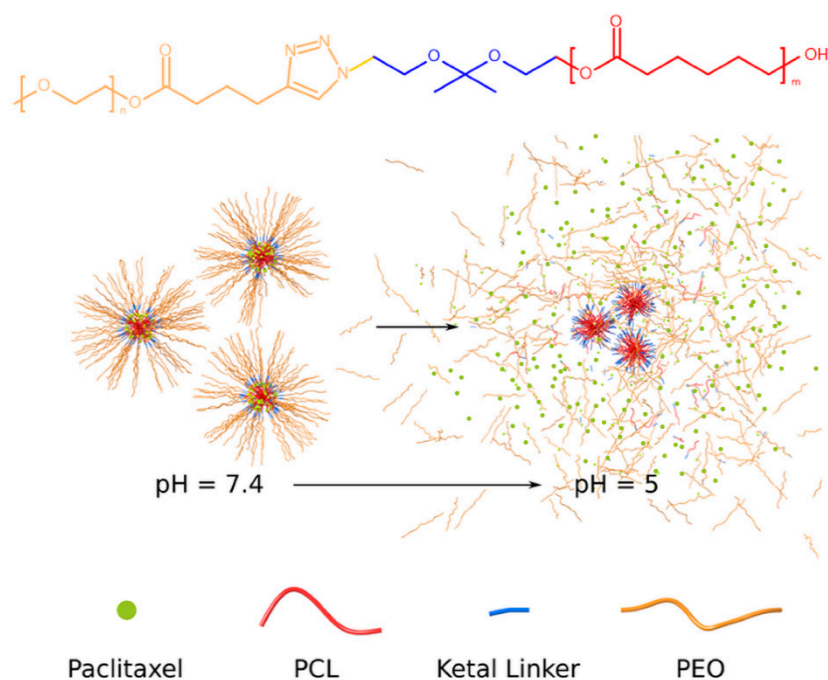


Figure 1. Chemical structure of the pH-triggered acid-labile block copolymer MPEO₄₄-*b*-PCL₁₇ (top) and the schematic nanoparticles assembly/disassembly mechanism at pH ~5.0 (bottom).

2. Materials and Methods

2.1. Materials

Chemicals were purchased from Sigma-Aldrich at the highest purity and, if not stated otherwise, were used as received.

2.2. Synthesis of MPEO₄₄-*b*-PCL₁₇ Diblock Copolymer Containing a Ketal Group

The synthesis and characterization of MPEO-*b*-PCL diblock copolymer are described in our previous publication [29]. Briefly, a seven-step synthetic method that combines carbodiimide chemistry (DCC method), a “click” reaction, and ring-opening polymerization (ROP) was employed to successfully produce a series of MPEO-*b*-PCL diblock copolymers (herein referred to as MPEO₄₄-*b*-PCL₁₇). Firstly, through a four-step pathway containing different synthetic routes, the low-molecular-weight compounds were prepared, further used as precursors for constructing the acid-labile ketal group. Then the block copolymers were synthesized in the next three steps via a DCC method, “click” reactions, and ROP (Supplementary Materials, Figure S1).

2.3. Characterisation Techniques

¹H NMR and ¹³C NMR spectra (300 MHz, respectively) were recorded using a Bruker Avance DPX 300 NMR spectrometer with CDCl₃ as the solvent at 25 °C. The chemical shifts were relative to TMS using hexamethyldisiloxane (HMDSO, $\delta = 0.05$ and 2.0 ppm from TMS in ¹H NMR and ¹³C NMR spectra) as the internal standard.

The number-average molecular weights (M_n), weight-average molecular weights (M_w), and dispersities (M_w/M_n) of the synthesized macromer, macroinitiator, and final block copolymer were determined by size exclusion chromatography (SEC). SEC analysis was performed using an SDS 150 pump (Watrex, Carolina Centrum, Czech Republic) equipped with refractometric (Shodex RI-101, Tokyo, Japan) and UV (Watrex UVD 250, Carolina Centrum, Czech Republic) detectors. The separation system consisted of two PLgel MIXED-C columns (Polymer Laboratories, Cambridge, UK) and was calibrated with polystyrene standards (PSS, Esslingen, Germany). THF was used as the mobile phase at a flow rate of 1.0 mL·min⁻¹ at 25 °C. Data collection and processing were performed using the Clarity software package.

The DLS measurements were performed using an ALV CGE laser goniometer consisting of a 22 mW HeNe linear polarized laser operating at a wavelength ($\lambda = 632.8$ nm), an ALV 6010 correlator, and a pair of avalanche photodiodes operating in pseudo-cross-correlation mode. The samples were loaded into 10 mm diameter glass cells and maintained at 37 ± 1 °C. The data were collected using the ALV Correlator Control software and the counting time was 45 s. The measured intensity correlation functions $g_2(t)$ were analyzed using the algorithm REPES (incorporated in the GENDIST program) [38], resulting in the distributions of relaxation times shown in equal area representation as $\tau A(\tau)$. The mean relaxation time or relaxation frequency ($\Gamma = \tau^{-1}$) is related to the diffusion coefficient (D) of the nanoparticles as $D = \frac{\Gamma}{q^2}$ where $q = \frac{4\pi n \sin \frac{\theta}{2}}{\lambda}$ is the scattering vector being n the refractive index of the solvent and θ the scattering angle. The hydrodynamic radius (R_H) or the distributions of R_H were calculated by using the Stokes-Einstein relation:

$$R_H = \frac{k_B T}{6\pi\eta D} \quad (1)$$

where k_B is the Boltzmann constant, T the absolute temperature, and η the viscosity of the solvent.

In the static light scattering (SLS), the scattering angle was varied from 30° to 150° with a 10° stepwise increase. The absolute light scattering is related to weight-average molar mass ($M_{w(NP)}$) and to the radius of gyration (R_G) of the nanoparticles by the Zimm formalism represented as:

$$\frac{K_c}{R_\theta} = \frac{1}{M_{w(NP)}} \left(1 + \frac{R_G^2 q^2}{3} \right) \quad (2)$$

where K is the optical constant, which includes the square of the refractive index increment (dn/dc), R_θ is the excess normalized scattered intensity (toluene was applied as standard solvent), and c is the polymer concentration given in mg mL^{-1} . The refractive index increment (dn/dc) of the MPEO₄₄-*b*-PCL₁₇ NPs in PBS (0.140 g L^{-1}) was determined using a Brice-Phoenix differential refractometer operating at $\lambda = 632.8$ nm.

The average ζ -potential of the NPs was performed using a Zetasizer Nano-ZS, Model ZEN3600 Instrument (Malvern Instruments, Malvern, UK). The equipment measures the electrophoretic mobility (U_E) and converts the value into ζ -potential (mV) through Henry's equation (Equation (3)) where ϵ is the dielectric constant of the medium and $f(ka)$ is Henry's function calculated through the Smoluchowski approximation with $f(ka) = 1.5$ which was calculated using the DTS (Nano) program.

$$U_E = \frac{2\epsilon\zeta f(ka)}{3\eta} \quad (3)$$

The small-angle X-ray scattering (SAXS) experiments were performed on the P12 BioSAXS beamline at the PETRA III storage ring of the Deutsche Elektronen Synchrotron (DESY, Hamburg, Germany) at 20 °C using a Pilatus 2M detector (Dectris, Baden, Switzerland) and synchrotron radiation with a wavelength of $\lambda = 0.1$ nm. The sample-detector distance was 3 m, allowing for measurements in the q -range interval from 0.11 to 4.4 nm^{-1} . The q -range was calibrated using the diffraction patterns of silver behenate. Background scattering of the solvent was carefully subtracted. We have used SASFit software [39,40] and the combination of two models to describe the scattering behavior of nanoparticles. The expression for the sphere with gaussian chains attached has been derived by Pedersen and Gerstenberg [41,42]. Equation (4) for generalized Gaussian coil is as follow:

$$I(q) = I_0 \left(\frac{1}{\nu U^{\frac{1}{2\nu}}} \gamma \left(\frac{1}{2\nu}, U \right) - \frac{1}{\nu U^{\frac{1}{\nu}}} \gamma \left(\frac{1}{\nu}, U \right) \right) \quad (4)$$

where $U = (2\nu + 1)(2\nu + 2)\frac{q^2 R_g^2}{6}$; ν is the excluded volume parameter from the Flory mean-field theory.

Transmission electron microscopy (TEM) analysis was carried out on a Tecnai G2 Spirit Twin at 120 kV (FEI, Lausanne, Switzerland).

2.4. Nanoparticle (NP) Preparation

A preheated (40 °C) acetone solution (2.0 mL) containing the MPEO₄₄-*b*-PCL₁₇ block copolymer (5.0 mg) and the chemotherapeutic PTX (0.1 mg) was added drop-wise (EW-74900-00, Cole-Parmer®) into a pre-heated (40 °C) PBS solution (4 mL, pH ~7.4). The pre-formed NPs were allowed to self-assemble, and then the solvent was evaporated under reduced pressure. The final concentration was adjusted to 1 mg·mL⁻¹ (NPs) using PBS at pH ~7.4.

2.5. Drug Loading and Drug Loading Efficiency

PTX loaded into the NPs was measured by HPLC (Shimadzu, Japan) using a reverse-phase column Chromolith Performance RP-18e (100 × 4.6 mm², eluent water-acetonitrile with acetonitrile gradient 0–100 vol %, flow rate = 1.0 mL·min⁻¹). Firstly 100 µL of the drug-loaded NPs was collected from the bulk sample, filtered (0.45 µm), and diluted to 900 µL with Acetonitrile (Lach-ner, Neratovice, Czech Republic). Such procedure led to NPs dissolution. Afterward, 20 µL of the final sample was injected through a sample loop. PTX was detected at 227 nm using ultraviolet (UV) detection. The drug-loading content (LC) and the drug-loading efficiency (LE) were calculated by using the following equations:

$$LC(\%) = \frac{\text{drug amount in nanoparticles}}{\text{mass of nanoparticles}} \times 100 \quad (5)$$

$$LE(\%) = \frac{\text{drug amount in nanoparticles}}{\text{drug feeding}} \times 100 \quad (6)$$

2.6. Drug Release Experiments

The in vitro release of PTX from the block copolymer NPs was studied in pH-adjusted release media (pH ~7.4 and ~5.0) at 37 °C. Aliquots (500 µL) of drug-loaded block copolymer NPs in PBS were loaded into 36 Slide-A-Lyzer MINI dialysis microtubes with MWCO 10,000 (Pierce, Rockford, IL, USA). These microtubes were dialyzed against 4 L of pH-adjusted PBS buffer gently stirred. The drug release experiments were done in triplicate. At each sampling time, it was removed three microtubes from the dialysis system, and 300 µL from each microtube was sampled and diluted to 1.0 mL by using Acetonitrile (Lach-ner, Czech Republic). The PTX content at each sampling time was then determined via HPLC by applying the same procedure used to determine LC and LE.

2.7. Cell Culture and In Vitro Experiments

All HeLa cells experiments were performed according to the protocol used in our previously published paper [43]. Briefly, the HeLa cells were cultivated in Dulbecco's Modified Eagle's Medium (DMEM) supplemented with 10% fetal calf serum, 100 units of penicillin, and 100 µg·mL⁻¹ of streptomycin (Life Technology, Waltham, MA, USA). The cells were grown in a humidified incubator at 37 °C with 5% CO₂. For the cytotoxicity assay, 5000 cells per well were seeded in duplicates in 96 flats bottoms well plates in 100 µL of media 24 h before adding the NPs. For adding of the particles, the volume was calibrated to 80 µL, and 20 µL of the five times concentrated dilution of PTX or particle dispersion were added per well to a final PTX concentration ranging from 10⁻⁵ to 5 µg·mL⁻¹. All dilutions were made in full incubation medium under thorough mixing of each dilution step. The sample concentrations of the PTX-loaded particles were adjusted to contain the same total amount of PTX as the samples with free PTX. The cells were incubated with the free drug or NPs for 24 h or 48 h. Then 10 µL of alamarBlue® cell viability reagent (Life

Technologies, Waltham, MA, USA) were added to each well and incubated a minimum for 3 h at 37 °C. The fluorescence of the reduced marker dye was read with a Synergy H1 plate reader (BioTek Instruments, Winooski, VT, USA) at excitation 570 and emission 600 nm. The fluorescence intensity of the control samples (with no drug or particles added) was set as a marker of 100% cell viability. The fluorescence signal of “0% viability samples” (where all cells were killed by the addition of hydrogen peroxide) was used as background and subtracted from all values prior to calculations. The non-toxic character of the blank particles without drug was shown by incubation of cells up to 0.67 mg·L⁻¹ of blank particles. This corresponds to the amount of polymer that is contained in the samples of drug-loaded particles with 5 µg·L⁻¹ total PTX content. For the cell experiments, the PTX-dilutions in incubation medium were made from a PTX stock solution of 120 µg·mL⁻¹ in PBS/DMSO (96.5: 3.5 v/v) [44]. Precipitation of the hydrophobic PTX out of the cell culture medium can therefore be excluded because the PTX was previously fully dissolved in a PBS/DMSO solution (96.5: 3.5 v/v) and subsequently diluted in the serum-supplied medium under thorough mixing. Consequently, even at maximal PTX-concentration of 5 µg·mL⁻¹, the final DMSO concentration in the incubation medium was below 0.2% and, therefore, no effect on cell vitality in the applied setup [42,43]. All the cell experiments were the average of at least 4 measurements ($n \geq 4$).

3. Results and Discussion

A multi-synthetic pathway was developed in order to obtain well-defined acid-labile self-assemble copolymer NPs, which could release hydrophobic drugs at an increased rate at relevant mild acidic conditions. Due to careful selection of macromolecular characteristics, such as the molecular weight and the relative block length, the MPEO₄₄-*b*-PCL₁₇ block copolymer self-assembles in PBS (pH ~7.4), forming spherical NPs with a bulky core capable of encapsulating and controlling the release of the hydrophobic chemotherapeutic drug-PTX. This should raise potential PTX toxicity to cancer cells, while after releasing the cargo, the nanocarriers are further disassembled into environmentally neutral degradation products (Figure 1, bottom).

The chemical structure, composition, molecular weight, and dispersity of the obtained MPEO₄₄-*b*-PCL₁₇ block copolymer were confirmed by ¹H and ¹³C NMR spectroscopy (see Supplementary Materials, Figure S2) and SEC chromatography (Figure S3, black curve), as well. The macromolecular characteristics of the block copolymer are listed in Table 1.

Table 1. Macromolecular characteristics of the MPEO₄₄-*b*-PCL₁₇ block copolymer.

Sample	M_n^a (theor.) (g mol ⁻¹)	M_n^b (NMR) (g mol ⁻¹)	M_n^c (SEC) (g mol ⁻¹)	M_w/M_n^d (SEC)
MPEO ₄₄ - <i>b</i> -PCL ₁₇	4000	4200	3130	1.45

^a $M_n = [M]_0/[I]_0 \times 114 + M_n$ α -methoxy- ω -hydroxy-MPEO containing a ketal group (Supplementary Materials, Figure S2). ^b M_n was calculated by ¹H NMR spectroscopy [29]. ^c M_n and ^d M_w/M_n values are relative to PS standards (Supplementary Materials, Figure S3).

The acid-responsive degradation of the MPEO₄₄-*b*-PCL₁₇ block copolymer linkage at pH ~5.0 for 48 h was studied in detail by SEC analysis (Supplementary Materials, Figure S3 red curve) and ¹³C NMR spectroscopy (Supplementary Materials, Figure S4). The SEC chromatogram of the diblock copolymer before and after hydrolytic degradation, as indicated by the overlap of the SEC traces (see Figure S3, ESI), showed the full disappearance of the chromatogram due to the parent copolymer (Supplementary Materials, Figure S3, black curve). Two major populations have been formatted, corresponding to the PEO and PCL homopolymer species upon the cleavage of ketal linkage at the block junctions in acidic pH, respectively (Supplementary Materials, Figure S3 red curve). Besides, the cleavage of the ketal group under acidic conditions in the composition of MPEO₄₄-*b*-PCL₁₇ diblock copolymer confirmed by ¹³C NMR spectroscopy (Supplementary Materials, Figure S4), as was demonstrated in our previous paper [29]. However, the performed analyzes showed

strong evidence for the high selectivity of the hydrolysis towards the ketal group linker of the diblock, and no hydrolytic degradation of the PCL backbone was observed over the period mentioned above.

After solubilization in acetone, the MPEO₄₄-*b*-PCL₁₇ diblock copolymer underwent nanoprecipitation and self-assembled into spherical NPs in PBS, encapsulating the PTX chemotherapeutic (see, Section 2). The SLS and DLS data revealed the assembly of well-defined NPs after acetone evaporation (Figure 2). The linear relationship resulted from the plot of the relaxation frequency (Γ) versus the square of the scattering vector (q^2) (Figure 2a), which indicates the behavior of Brownian diffusion from spherical particles. Using the slope of the diffusion coefficient and employing the Stokes-Einstein equation (Equation (1), Mat. and Methods), an apparent R_H of 32.1 nm was estimated, which was in good agreement with the particle size measured at a fixed angle of 90° (Figure 2b).

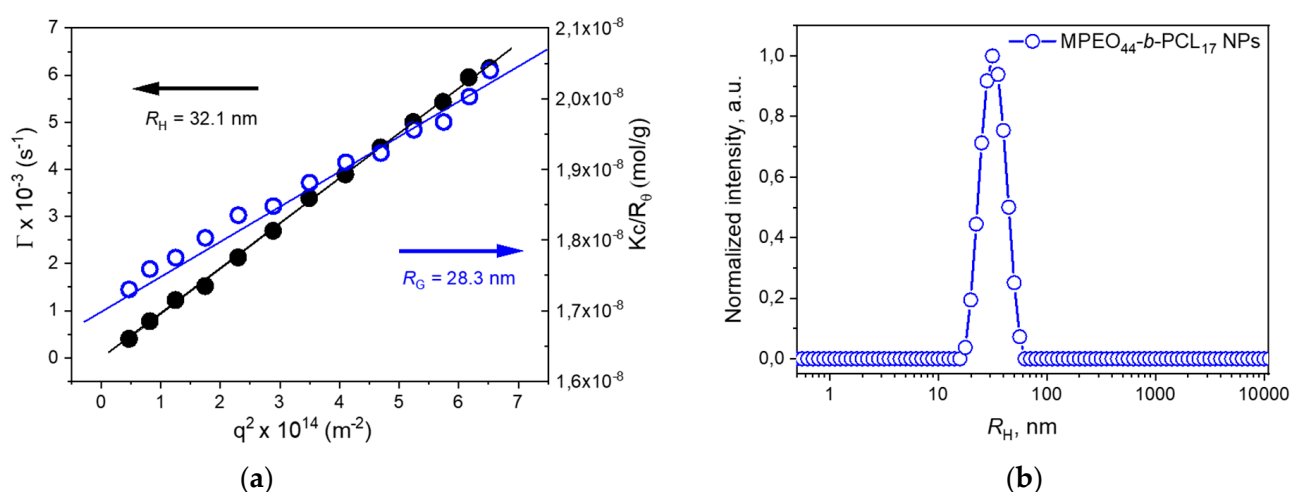


Figure 2. Measurement of angular dependence by DLS (●) and SLS (○) of the MPEO₄₄-*b*-PCL₁₇ NPs prepared using the nanoprecipitation protocol (a) and normalized intensity size distribution of the MPEO₄₄-*b*-PCL₁₇ NPs measured at angle 90° at a concentration of 1,0 mg·mL⁻¹ in PBS (pH ~7.4) and at 37 °C (b).

From the Zimm analysis of the SLS data (see Section 2), the values of the radius of gyration (R_G) were determined from the slope of the curve as being equal to 28.3 nm, and from the inverse of the intercept, the values of the NPs molecular weight ($M_w(\text{NP}'s)$) were determined as being equal to 2.9×10^7 g mol⁻¹. The aggregation number of the NPs (N_{agg}) were then calculated as $N_{\text{agg}} = M_w(\text{NP}'s)/M_w(\text{SEC}) = 9265$ chains being compatible with N_{agg} related in literature for MPEO-*b*-PCL NPs [45].

It is well established that the R_G/R_H ratio may provide qualitative information related to the architecture of the self-assemblies in the solution. The obtained R_G/R_H ratio was equal to 0.88, which is higher than that predicted for homogenous sphere (0.77) and was compatible with the formation of spherical block copolymer NPs with solvated shells [18,46]. The average ζ -potential of the studied self-assemble block copolymer NPs performed at pH 7.4 (PBS buffer, 0.01M) was close to neutrality (~0.5 mV) which indicates that particles were sterically stabilized by the PEO hydrophilic shell.

Thermodynamically stable polymeric NPs with a hydrodynamic diameter ($2R_H = D_H$) of ~64 nm were obtained. These NPs were perfectly suited for drug delivery by specific accumulation in solid tumor tissue by the EPR effect. The optimal particle size for the EPR effect is usually stated to be ~20 to 70 nm [47]. Moreover, another previously mentioned valuable target in cancer therapy is the acidic environment in endosomal (pH ~5.0 to ~6.0) and lysosomal (pH ~4.0 to ~5.0) compartments. Therefore, the degradation behavior of the polymer NPs containing the acid-labile ketal group was evaluated under acidic physiological conditions (pH ~5.0; at 37 °C) using DLS, SAXS, and TEM.

The DLS data from NPs measurements over 48 h at pH ~ 7.4 and ~ 5.0 are depicted in Figure 3. The DLS data clearly demonstrated that the hydrodynamic radius (R_H) of NPs remains unchanged at pH ~ 7.4 for 48 h (black circles, Figure 3a), whereas it continuously increased at pH ~ 5.0 over the 48 h (blue circles, Figure 3a). Additionally, we also observed the appearance of a scattering population that increased over time, that corresponded to smaller sizes fraction with $R_H \sim 2$ to 15 nm (blue circles, Figure 3a). A representative average intensity distribution of the NPs after 48 h at pH ~ 7.4 and ~ 5.0 are shown in Figure 3b. In contrast to the unimodal average size distribution of the NPs at pH ~ 7.4 (black circles, Figure 3b), the NPs average size distribution at pH ~ 5.0 is bimodal and shows two main population of particles with $R_H \sim 15$ nm and $R_H \sim 58$ nm (blue circles, Figure 3b), respectively.

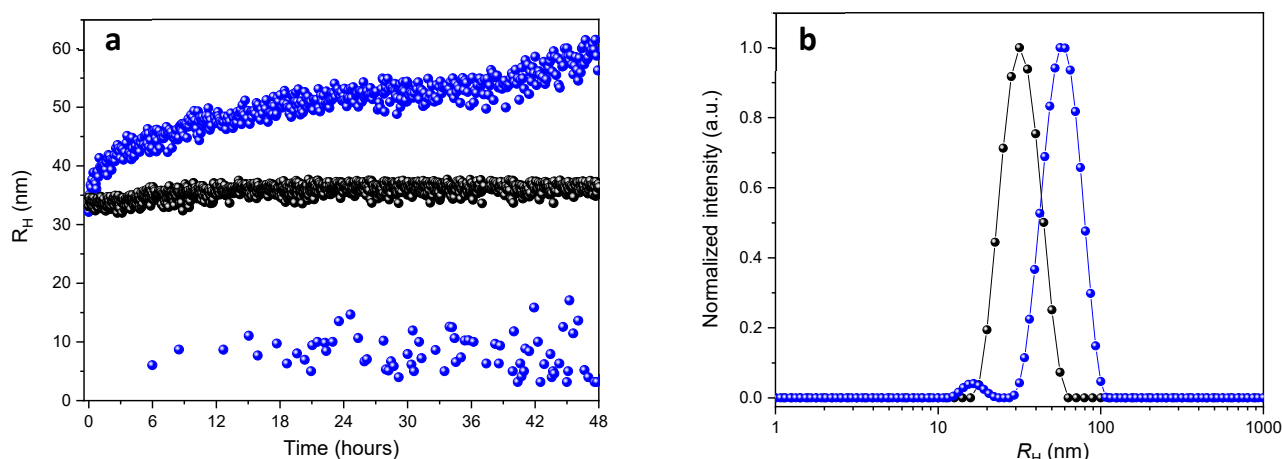


Figure 3. R_H evolution (a) and intensity distribution (b) measured by DLS at pH ~ 7.4 (●) and pH ~ 5.0 (●) for the MPEO₄₄-*b*-PCL₁₇ NPs after 48 h.

Moreover, the changes in the NPs inner structure under degradation were also evaluated by SAXS (Figure 4). The scattering curves were modeled using a combination of core-shell and Gaussian coil model (see Section 2). The parameters extracted from the SAXS curve fittings were radius of the core (R), the radius of gyration of the shell ($R_{g_{shell}}$), and the radius of gyration of the gaussian chains ($R_{g_{gauss}}$) for the particles and random coils in the solution, respectively. The values found at pH ~ 7.4 were $R = 23.4$ nm and $R_{g_{shell}} = 1.1$ nm, resulting in a total particle radius ($R + R_{g_{shell}}$) of 24.5 nm, which was only slightly smaller than the R_g determined through static light scattering ($R_G = 28.3$, Figure 2a). However, the profile of the scattering curve changes drastically after degradation at pH ~ 5.0 (Figure 4a). It was observed a reduction in the scattering intensity $I(q)$ at the zero scattering angle $I(0)$ and an increase in the scattering intensity in the high- q region (blue circles, Figure 4a), which indicated a decrease in the particle's molecular weight and the appearance of a scattering population of free chains analogous to that observed by DLS. In this case, the values found at pH ~ 5.0 were $R = 19.5$ nm, $R_{g_{shell}} = 5.6$ nm, and $R_{g_{gauss}} = 3$ nm for the spherical and Gaussian coil model, respectively. The overall reduction in the dimension of the particles after incubation at pH ~ 5.0 was confirmed by the shift on the distribution function $p(R)$ from the sphere model to lower values (Figure 4b). Furthermore, the increasing of $R_{g_{shell}}$ value, as well as the appearance of the free gaussian chains in solution, indicates, respectively, the increased swelling of the NPs shell and the release of MPEG from the NPs surface.

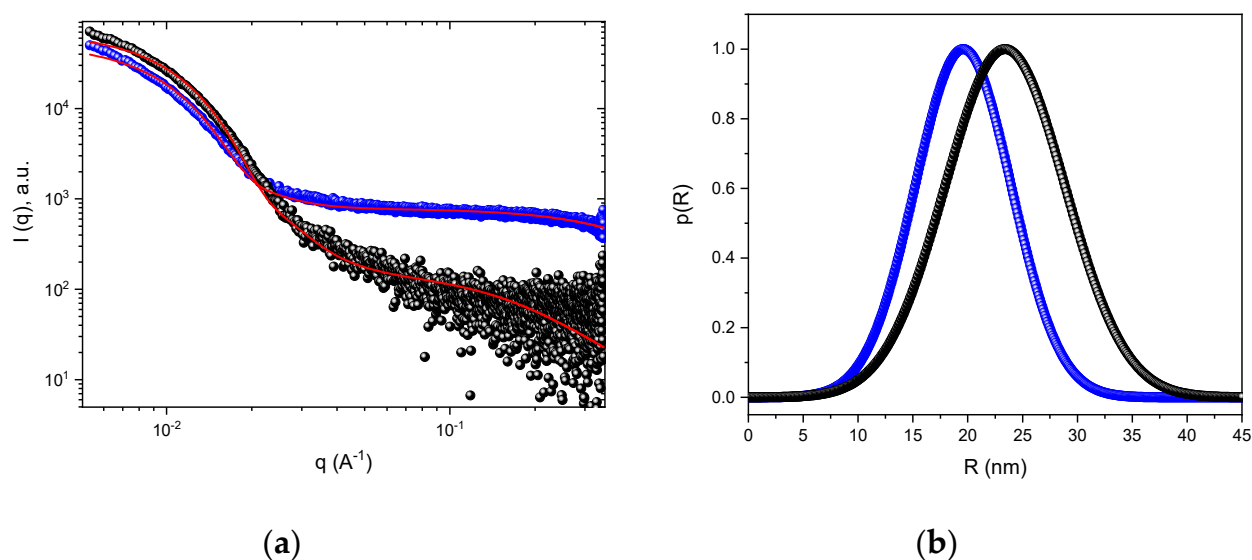


Figure 4. SAXS patterns of NPs after 48 h of incubation at pH ~ 7.4 (●) and pH ~ 5.0 (●) along to the fitting results—olid red lines (a) and the respective $p(R)$ vs. R profiles (b).

The overall scattering changes observed confirmed the sensitivity of the NPs to degradation under acidic conditions [29] and provide important information concerning the degradation process (Table 2). The appearance of distinct populations of particles along the time at pH ~ 5.0 seemed to be related to a continuous disassembly and aggregation process of the NPs after the hydrolysis of the ketal group [18]. Taking into consideration that the ketal group was preferentially localized at the NPs interface, between the PCL core and the PEO shell, the hydrolysis of the ketal group released the PEO chains from the NPs surfaces, increasing the NPs hydrophobicity, which induced its disassembly and aggregation. Therefore, the results obtained by DLS showed an increase in the NPs size from ~ 64 to ~ 116 nm, as well as the appearance of the scattering population at the smaller sizes between ~ 4 to ~ 30 nm. This is probably due to disassembled/aggregated NPs and the released of free PEO chains, respectively. (Figure 3). Likewise, this was observed by SAXS by the decrease in size and scattering component that describes the NPs and the increase in concentration of the free PEO chains. Similarly, the TEM images (Figure 5) showed a comparable increase in the size of the MPEO₄₄-*b*-PCL₁₇ block copolymer NPs at pH ~ 5.0 (Figure 5b) when compared to the NPs at pH ~ 7.4 (Figure 5a) after 24 h, which confirms that after degradation only undefined aggregates and disassembled NPs with free MPEO chains coexisted in solution.

Table 2. Structural features of the prepared MPEO₄₄-*b*-PCL₁₇ block copolymer nanoparticles before (pH ~ 7.4) and after (pH ~ 5.0) degradation.

NPs	R_H^a	R_G^b	R^c	$R_{g_{shell}}^c$	$R_{g_{gauss}}^c$
MPEO ₄₄ - <i>b</i> -PCL ₁₇ (pH ~ 7.4)	32.1	28.3	23.4	1.1	-
MPEO ₄₄ - <i>b</i> -PCL ₁₇ (pH ~ 5.0)	15 and 58	-	19.5	5.6	3.0

^a DLS; ^b SLS; ^c SAXS; Values are given in nm.

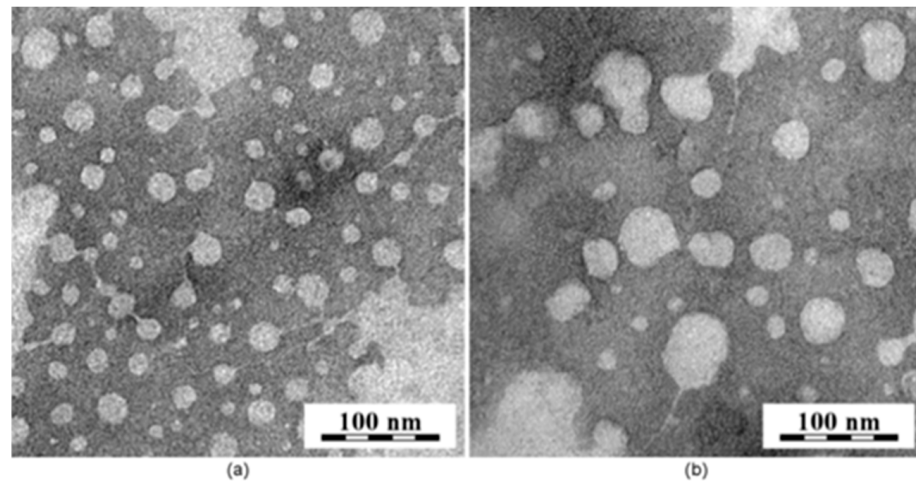


Figure 5. TEM images of MPEO₄₄-*b*-PCL₁₇ at pH ~7.4 (a) and pH ~5.0 (b) after 48 h incubation.

The release profile of the chemotherapeutic PTX was explored towards mimicking the target acidic environment in endosomal and lysosomal compartments (pH ~5.0, 37 °C) (Figure 6). Furthermore, to simulate physico-chemical conditions during transport in the blood and in normal healthy tissues, the release experiments at pH ~7.4 and 37 °C were also performed, as well (Figure 5). The obtained results suggest that the acid pH accelerates the release of the drug from the NPs, most likely due to the NPs physical destabilization (pH-triggered disassembly-aggregation, Figure 3). The drug cargo was released almost twice as efficiently (~70% released) within 48 h at pH ~5.0 (mimicking intracellular environment) than at physiological conditions of pH ~7.4. On the other hand, at pH ~7.4, only ~36% of the drug-loaded into the NPs cores was released.

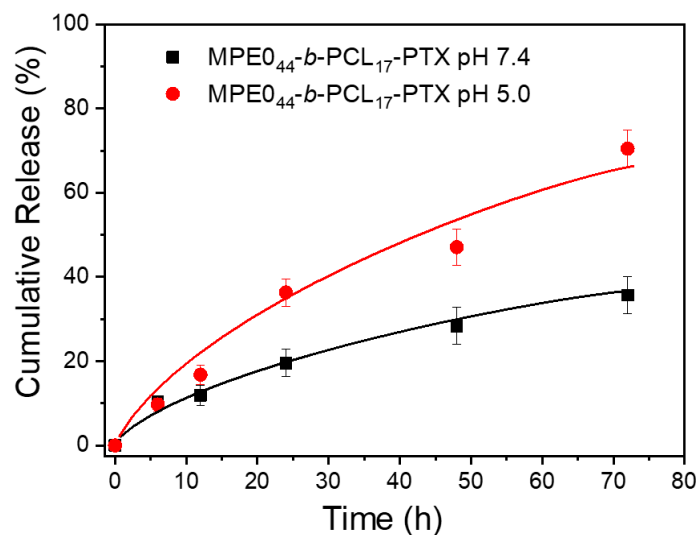


Figure 6. Paclitaxel release profiles from MPEO₄₄-*b*-PCL₁₇-PTX NPs at pH ~7.4 (■) and pH ~5.0 (●).

The drug-release profile was considered not optimal; however, a yet faster release was expected in contact with more complex media such as the serum-supplied cell culture medium. To investigate the inhibitory effect on tumor cells, the MPEO₄₄-*b*-PCL₁₇ NPs were loaded with the antitumor drug PTX with an overall cargo rate of around 2.0 wt% (loading efficiency of 92%, see Section 2). Given the hydrophobicity of the NPs core and the PTX (negligible free PTX was observed), no additional purification step was carried out. The cell viability assay was used to document in vitro cytotoxicity as a classical approach to evaluate the direct effect of the drug carrier NPs on target cancer cells. The HeLa cell line was selected as a widely used and well-studied cancer cell model system [47]. The drug-loaded NPs

were incubated with the HeLa cells, and the *in vitro* cytotoxicity after 24 h and 48 h of incubation was assessed by alamarBlue[®] assay (Figure 7). After 48 h incubation with the cells, the PTX-loaded MPEO₄₄-*b*-PCL₁₇ NPs exhibited significantly stronger toxicity than the free drug (Figure 7b). In contrast, the drug-free NPs showed only negligible cytotoxicity to the cancer cells (Supplementary Materials, Figure S5). This increased cytotoxicity of the drug-carrying NPs compared to the free drug was supposedly owed to endocytotic uptake [48]; at low drug concentrations (below 1 $\mu\text{g}\cdot\text{mL}^{-1}$, see Figure 7b), the endocytotic uptake of the drug-loaded nanocarriers would be more efficient than the uptake of the free drug into the cells. With increasing drug concentration, this effect became less prominent (see Figure 7b). Once internalized via endocytosis, the PTX-loaded nanocarriers swiftly and efficiently released their cargo when the enzymes and acidic conditions in endosomes triggered the cleavage of the pH-sensitive acyclic ketal bond [43,44]. Drug-free MPEO₄₄-*b*-PCL₁₇ NPs were also tested up to the applied maximal concentration (0.67 $\text{mg}\cdot\text{mL}^{-1}$) with no significant cytotoxic activity (Figure S5). Last but not least, the negligible toxicity of the unloaded-MPEO₄₄-*b*-PCL₁₇ NPs emphasized that the presented nanocarrier system produced no toxic degradation products, and at any rate, the products (PCL and PEO) are well-known and FDA-approved as environmentally friendly blocks.

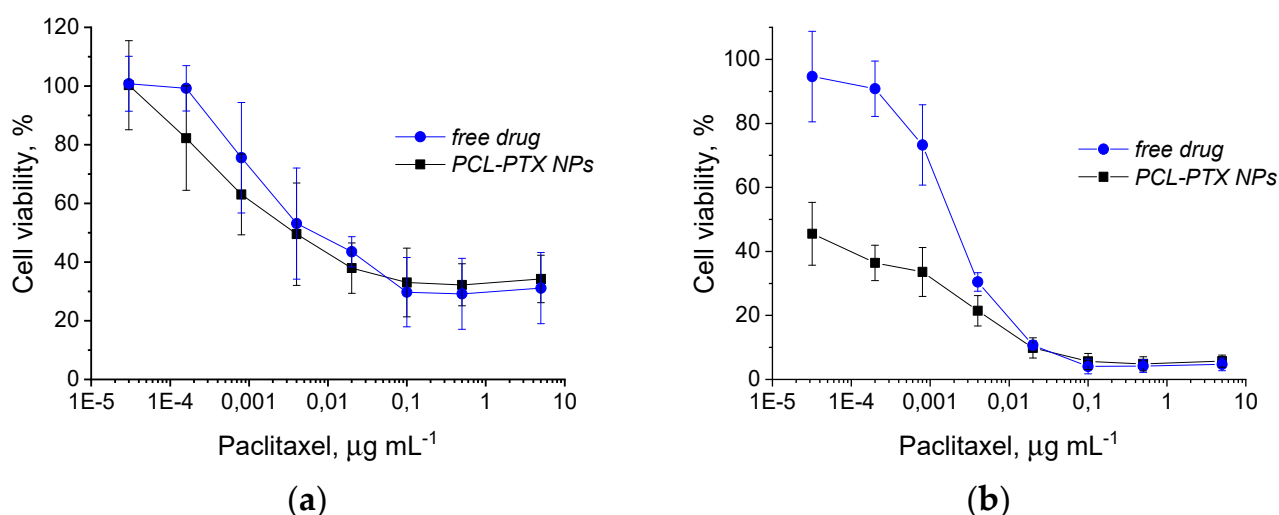


Figure 7. Viability of HeLa cells after 24 h (a) and 48 h (b) of incubation with different concentrations of free PTX (blue circles) and PTX-loaded MPEO₄₄-*b*-PCL₁₇ NPs (black squares).

4. Conclusions

In summary, well-defined nanoparticles prepared by the self-assembly of the new amphiphilic MPEO₄₄-*b*-PCL₁₇ block copolymer in an aqueous solution were presented. The NPs structure was characterized in detail by DLS, SLS, SAXS, and TEM. On decreasing pH the acid-labile ketal linker enabled the disassembly of the nanoparticles in a buffer that simulated the acidic environment in endosomal and lysosomal compartments. As a result, the chemotherapeutic paclitaxel was released, and the polymer particles disintegrated into neutral degradation products as confirmed by SEC, ¹³C NMR, and by *in vitro* cell viability tests, as well. In addition, the *in vitro* cell viability experiments demonstrated the great potential of the pH-triggered NPs as a drug-delivery system in cancer therapy; the *in vitro* cytotoxicity studies showed an important increase in activity of the NP-loaded with drug and the free-drug NPs are degraded into well-known, and FDA-approved by-products and itself introduced no toxicity to cells. The particle's hydrophilic surface coat and size below the cut-off size of the leaky pathological vasculature (NPs < 100 nm) predetermined the NPs for long circulation and efficient accumulation in solid tumors due to the EPR effect and together with the ability to release a drug at the endosomal pH with concomitant high cytotoxicity makes them suitable candidates for cancer therapy.

Supplementary Materials: The following are available online at <https://www.mdpi.com/article/10.3390/polym13091465/s1>, Figure S1: Synthetic route for the preparation of MPEO-*b*-PCL diblock copolymers, Figure S2: ¹H (left) and ¹³C (right) NMR spectra of the MPEO₄₄-*b*-PCL₁₇ diblock copolymer in CDCl₃, Figure S3: SEC chromatograms in THF of MPEO₄₄-*b*-PCL₁₇ diblock copolymer (black line), α -methoxy- ω -hydroxy-poly(ethylene oxide) macromer containing a ketal group (blue line) and the MPEO₄₄-*b*-PCL₁₇ diblock copolymer after degradation (phosphate buffer saline) at pH ~5.0 for 48h (red line). Figure S4: ¹³C NMR spectra of MPEO₄₄-*b*-PCL₁₇ diblock copolymer (top) before degradation and (bottom) after degradation, Figure S5: Cell viability of HeLa cell line after 24 h (black squares) and 48 h (red circles) incubation with different concentrations of drug-free MPEO₄₄-*b*-PCL₁₇ diblock copolymer NPs.

Author Contributions: S.L.P. conceived the idea for the synthesis of PEO-*b*-PCL diblock copolymer containing ketal group, performed the synthesis, and wrote the manuscript. E.J. prepared the nanoparticles, performed DLS/SLS experiments, analyzed DLS/SLS data, and wrote the manuscript. A.J. performed SEC analysis and analyzed SEC data, and wrote the manuscript. A.H. and O.J. performed the biological experiments with HeLa cells. A.Z. performed the SAXS experiments and data analysis. R.K. performed NMR experiments. E.P. performed the TEM experiment, M.H. supervised the work. All authors have read and agreed to the published version of the manuscript.

Funding: This work was supported by Czech Science Foundation (Grant # 20–15077Y) and (Grant # 20-13946Y). M.H. thanks the Ministry of Education, Youth and Sports of the Czech Republic (grant INTER-COST # LTC19032).

Institutional Review Board Statement: Not applicable.

Informed Consent Statement: Not applicable.

Data Availability Statement: The data presented in this study are available on request from the corresponding author.

Conflicts of Interest: The authors declare no conflict of interest.

References

1. Allen, C.; Maysinger, D.; Eisenberg, A. Nano-engineering block copolymer aggregates for drug delivery. *Colloids Surf. B Biointerfaces* **1999**, *16*, 3–27.
2. Atanase, L.I.; Desbrieres, J.; Riess, G. Micellization of synthetic and polysaccharides-based graft copolymers in aqueous media. *Prog. Polym. Sci.* **2017**, *73*, 32–60. [[CrossRef](#)]
3. Lee, S.-W.; Yun, M.-H.; Jeong, S.W.; In, C.-H.; Kim, J.-Y.; Seo, M.-H.; Pai, C.-M.; Kim, S.-O. Development of docetaxel-loaded intravenous formulation, Nanoxel-PMTM using polymer-based delivery system. *J. Control. Release* **2011**, *155*, 262–271. [[CrossRef](#)]
4. Mikhail, A.S.; Allen, C. Block copolymer micelles for delivery of cancer therapy: Transport at the whole body, tissue and cellular levels. *J. Control. Release* **2009**, *138*, 214–223. [[CrossRef](#)] [[PubMed](#)]
5. Choucair, A.; Eisenberg, A. Control of amphiphilic block copolymer morphologies using solution conditions. *Eur. Phys. J. E* **2003**, *10*, 37–44. [[CrossRef](#)] [[PubMed](#)]
6. Atanase, L.; Riess, G. Self-assembly of block and graft copolymers in organic solvents: An overview of recent advances. *Polymers* **2018**, *10*, 62. [[CrossRef](#)]
7. Hrubý, M.; Etrych, T.; Kučka, J.; Forsteroová, M.; Ulbrich, K. Hydroxybisphosphonate-containing polymeric drug-delivery systems designed for targeting into bone tissue. *J. Appl. Polym. Sci.* **2006**, *101*, 3192–3201. [[CrossRef](#)]
8. Xiong, X.B.; Falamarzian, A.; Garg, S.M.; Lavasanifar, A. Engineering of amphiphilic block copolymers for polymeric micellar drug and gene delivery. *J. Control. Release* **2011**, *155*, 248–261. [[CrossRef](#)] [[PubMed](#)]
9. Li, H.-J.; Wang, H.-X.; Sun, C.-Y.; Du, J.-Z.; Wang, J. Shell-detachable nanoparticles based on a light-responsive amphiphile for enhanced siRNA delivery. *RSC Adv.* **2014**, *4*, 1961–1964. [[CrossRef](#)]
10. Bawa, K.K.; Jazani, A.M.; Ye, Z.; Oh, J.K. Synthesis of degradable PLA-based diblock copolymers with dual acid/reduction-cleavable junction. *Polymer* **2020**, *194*, 122391. [[CrossRef](#)]
11. Liu, Y.; Wang, W.; Yang, J.; Zhou, C.; Sun, J. pH-sensitive polymeric micelles triggered drug release for extracellular and intracellular drug targeting delivery. *Asian J. Pharm. Sci.* **2013**, *8*, 159–167. [[CrossRef](#)]
12. Kedar, U.; Phutane, P.; Shidhaye, S.; Kadam, V. Advances in polymeric micelles for drug delivery and tumor targeting. *Nanomed. Nanotechnol. Biol. Med.* **2010**, *6*, 714–729. [[CrossRef](#)]
13. Liu, Y.; Sun, J.; Cao, W.; Yang, J.; Lian, H.; Li, X.; Sun, Y.; Wang, Y.; Wang, S.; He, Z. Dual targeting folate-conjugated hyaluronic acid polymeric micelles for paclitaxel delivery. *Int. J. Pharm.* **2011**, *421*, 160–169. [[CrossRef](#)]
14. Imran Ul-haq, M.; Lai, B.F.L.; Kizhakkedathu, J.N. Hybrid polyglycerols with long blood circulation: Synthesis, biocompatibility, and biodistribution. *Macromol. Biosci.* **2014**, *14*, 1469–1482. [[CrossRef](#)]

15. Lin, W.; Ma, G.; Ji, F.; Zhang, J.; Wang, L.; Sun, H.; Chen, S. Biocompatible long-circulating star carboxybetaine polymers. *J. Mater. Chem. B* **2015**, *3*, 440–448. [[CrossRef](#)]
16. Gibson, M.I.; O'Reilly, R.K. To aggregate, or not to aggregate? considerations in the design and application of polymeric thermally-responsive nanoparticles. *Chem. Soc. Rev.* **2013**, *42*, 7204–7213. [[CrossRef](#)] [[PubMed](#)]
17. Jeanmaire, D.; Laliturai, J.; Almalik, A.; Carampin, P.; d'Arcy, R.; Lallana, E.; Evans, R.; Winpenny, R.E.P.; Tirelli, N. Chemical specificity in REDOX-responsive materials: The diverse effects of different reactive oxygen species (ROS) on polysulfide nanoparticles. *Polym. Chem.* **2014**, *5*, 1393. [[CrossRef](#)]
18. Giacomelli, F.C.; Stepánek, P.; Giacomelli, C.; Schmidt, V.; Jäger, E.; Jäger, A.; Ulbrich, K. pH-triggered block copolymer micelles based on a pH-responsive PDPA (poly[2-(diisopropylamino)ethyl methacrylate]) inner core and a PEO (poly(ethylene oxide)) outer shell as a potential tool for the cancer therapy. *Soft Matter* **2011**, *7*, 9316. [[CrossRef](#)]
19. Wang, Y.; Zhou, K.; Huang, G.; Hensley, C.; Huang, X.; Ma, X.; Zhao, T.; Sumer, B.D.; DeBerardinis, R.J.; Gao, J. A nanoparticle-based strategy for the imaging of a broad range of tumours by nonlinear amplification of microenvironment signals. *Nat. Mater.* **2014**, *13*, 204–212. [[CrossRef](#)]
20. Yin, H.; Lee, E.S.; Kim, D.; Lee, K.H.; Oh, K.T.; Bae, Y.H. Physicochemical characteristics of pH-sensitive poly(l-Histidine)-b-poly(ethylene glycol)/poly(l-Lactide)-b-poly(ethylene glycol) mixed micelles. *J. Control. Release* **2008**, *126*, 130–138. [[CrossRef](#)]
21. Qi, P.; Bu, Y.; Xu, J.; Qin, B.; Luan, S.; Song, S. pH-responsive release of paclitaxel from hydrazone-containing biodegradable micelles. *Colloid Polym. Sci.* **2017**, *295*, 1–12. [[CrossRef](#)]
22. Xu, J.; Luan, S.; Qin, B.; Wang, Y.; Wang, K.; Qi, P.; Song, S. Backbone-hydrazone-containing biodegradable copolymeric micelles for anticancer drug delivery. *J. Nanoparticle Res.* **2016**, *18*, 316. [[CrossRef](#)]
23. Guan, Y.; Su, Y.; Zhao, L.; Meng, F.; Wang, Q.; Yao, Y.; Luo, J. Biodegradable polyurethane micelles with pH and reduction responsive properties for intracellular drug delivery. *Mater. Sci. Eng. C* **2017**, *75*, 1221–1230. [[CrossRef](#)] [[PubMed](#)]
24. Pang, X.; Jiang, Y.; Xiao, Q.; Leung, A.W.; Hua, H.; Xu, C. pH-responsive polymer–drug conjugates: Design and progress. *J. Control. Release* **2016**, *222*, 116–129. [[CrossRef](#)] [[PubMed](#)]
25. Wang, B.; Xu, C.; Xie, J.; Yang, Z.; Sun, S. pH controlled release of chromone from chromone-Fe₃O₄ nanoparticles. *J. Am. Chem. Soc.* **2008**, *130*, 14436–14437. [[CrossRef](#)] [[PubMed](#)]
26. Hu, L.; Zhang, P.; Wang, X.; Cheng, X.; Qin, J.; Tang, R. pH-sensitive carboxymethyl chitosan hydrogels via acid-labile ortho ester linkage for potential biomedical applications. *Carbohydr. Polym.* **2017**, *178*, 166–179. [[CrossRef](#)]
27. Toncheva, V.; Schacht, E.; Ng, S.Y.; Barr, J.; Heller, J. Use of block copolymers of poly(ortho esters) and poly(ethylene glycol) micellar carriers as potential tumour targeting systems. *J. Drug Target.* **2003**, *11*, 345–353. [[CrossRef](#)]
28. Khaja, S.D.; Lee, S.; Murthy, N. Acid-degradable protein delivery vehicles based on metathesis chemistry. *Biomacromolecules* **2007**, *8*, 1391–1395. [[CrossRef](#)]
29. Petrova, S.; Jäger, E.; Konefał, R.; Jäger, A.; Venturini, C.G.; Spěváček, J.; Pavlova, E.; Štěpánek, P. Novel poly(ethylene oxide monomethyl ether)-b-poly(ϵ -caprolactone) diblock copolymers containing a pH-acid labile ketal group as a block linkage. *Polym. Chem.* **2014**, *5*, 3884–3893. [[CrossRef](#)]
30. Siepmann, J. Mathematical modeling of bioerodible, polymeric drug delivery systems. *Adv. Drug Deliv. Rev.* **2001**, *48*, 229–247. [[CrossRef](#)]
31. Atanase, L.I.; Riess, G. Micellization of pH-stimulable poly(2-vinylpyridine)-b-poly(ethylene oxide) copolymers and their complexation with anionic surfactants. *J. Colloid Interface Sci.* **2013**, *395*, 190–197. [[CrossRef](#)] [[PubMed](#)]
32. Iurciuc-Tincu, C.-E.; Cretan, M.S.; Purcar, V.; Popa, M.; Daraba, O.M.; Atanase, L.I.; Ochiuz, L. Drug delivery system based on pH-sensitive biocompatible poly(2-vinyl pyridine)-b-poly(ethylene oxide) nanomicelles loaded with curcumin and 5-fluorouracil. *Polymers* **2020**, *12*, 1450. [[CrossRef](#)] [[PubMed](#)]
33. Daraba, O.M.; Cadinoiu, A.N.; Rata, D.M.; Atanase, L.I.; Vochita, G. Antitumoral drug-loaded biocompatible polymeric nanoparticles obtained by non-aqueous emulsion polymerization. *Polymers* **2020**, *12*, 1018. [[CrossRef](#)] [[PubMed](#)]
34. Atanase, L.I. Micellar drug delivery systems based on natural biopolymers. *Polymers* **2021**, *13*, 477. [[CrossRef](#)] [[PubMed](#)]
35. Zhang, Y.; Cao, X.; Liang, T.; Tong, Z. Acid/light dual-responsive biodegradable polymeric nanocarriers for efficient intracellular drug delivery. *Polym. Bull.* **2019**, *76*, 1775–1792. [[CrossRef](#)]
36. Rieger, J.; Dubois, P.; Jérôme, R.; Jérôme, C. Controlled synthesis and interface properties of new amphiphilic PCL-g-PEO copolymers. *Langmuir* **2006**, *22*, 7471–7479. [[CrossRef](#)]
37. Kumar, N.; Ravikumar, M.N.V.; Domb, A.J. Biodegradable block copolymers. *Adv. Drug Deliv. Rev.* **2001**, *53*, 23–44. [[CrossRef](#)]
38. Jakeš, J. Testing of the constrained regularization method of inverting Laplace transform on simulated very wide quasielastic light scattering autocorrelation functions. *Czechoslov. J. Phys.* **1988**, *38*, 1305–1316. [[CrossRef](#)]
39. Brešler, I.; Kohlbrecher, J.; Thünemann, A.F. SASfit: A tool for small-angle scattering data analysis using a library of analytical expressions. *J. Appl. Crystallogr.* **2015**, *48*, 1587–1598. [[CrossRef](#)]
40. Pedersen, J.S. Form factors of block copolymer micelles with spherical, ellipsoidal and cylindrical cores. *J. Appl. Crystallogr.* **2000**, *33*, 637–640. [[CrossRef](#)]
41. Pedersen, J.S.; Gerstenberg, M.C. Scattering form factor of block copolymer micelles. *Macromolecules* **1996**, *29*, 1363–1365. [[CrossRef](#)]
42. Trivedi, A.B.; Kitabatake, N.; Doi, E. Toxicity of dimethyl sulfoxide as a solvent in bioassay system with HeLa cells evaluated colorimetrically with 3-(4,5-dimethylthiazol-2-yl)-2,5-diphenyl-tetrazolium bromide. *Agric. Biol. Chem.* **1990**, *54*, 2961–2966. [[CrossRef](#)] [[PubMed](#)]

43. Jäger, A.; Jäger, E.; Surman, F.; Höcherl, A.; Angelov, B.; Ulbrich, K.; Drechsler, M.; Garamus, V.M.; Rodriguez-Emmenegger, C.; Nallet, F.; et al. Nanoparticles of the poly([N-(2-hydroxypropyl)]methacrylamide)-b-poly[2-(diisopropylamino)ethyl methacrylate] diblock copolymer for pH-triggered release of paclitaxel. *Polym. Chem.* **2015**, *6*, 4946–4954. [[CrossRef](#)]
44. Dubikovskaya, E.A.; Thorne, S.H.; Pillow, T.H.; Contag, C.H.; Wender, P.A. Overcoming multidrug resistance of small-molecule therapeutics through conjugation with releasable octaarginine transporters. *Proc. Natl. Acad. Sci. USA* **2008**, *105*, 12128–12133. [[CrossRef](#)] [[PubMed](#)]
45. Šachl, R.; Uchman, M.; Matějček, P.; Procházka, K.; Štěpánek, M.; Špírková, M. Preparation and characterization of self-assembled nanoparticles formed by poly(ethylene oxide)-block-poly(ϵ -caprolactone) copolymers with long poly(ϵ -caprolactone) blocks in aqueous solutions. *Langmuir* **2007**, *23*, 3395–3400. [[CrossRef](#)] [[PubMed](#)]
46. Castro, C.E.D.; Mattei, B.; Riske, K.A.; Jäger, E.; Jäger, A.; Štěpánek, P.; Giacomelli, F.C. Understanding the structural parameters of biocompatible nanoparticles dictating protein fouling. *Langmuir* **2014**, *30*, 9770–9779. [[CrossRef](#)] [[PubMed](#)]
47. Rahbari, R.; Sheahan, T.; Modes, V.; Collier, P.; Macfarlane, C.; Badge, R.M. A novel L1 retrotransposon marker for HeLa cell line identification. *Biotechniques* **2009**, *46*, 277–284. [[CrossRef](#)] [[PubMed](#)]
48. Li, D.; Zhang, Y.; Jin, S.; Guo, J.; Gao, H.; Wang, C. Development of a redox/pH dual stimuli-responsive MSP@P(MAA-Cy) drug delivery system for programmed release of anticancer drugs in tumour cells. *J. Mater. Chem. B* **2014**, *2*, 5187–5194. [[CrossRef](#)] [[PubMed](#)]